Distinct levels in Pom1 gradients limit Cdr2 activity and localization to time and position division

Payal Bhatia, Olivier Hachet, Micha Hersch, Sergio A. Rincon, Martine Berthelot-Grosjean, Sascha Dalessi, Laetitia Basterra, Sven Bergmann, Anne Paoletti, Sophie G. Martin

Cell Cycle 13:4, 538–552; February 15, 2014; © 2014 Landes Bioscience

Distinct levels in Pom1 gradients limit Cdr2 activity and localization to time and position division

Payal Bhatia[1], Olivier Hachet[1,†], Micha Hersch[2,3,†], Sergio A Rincon[4,5,†], Martine Berthelot-Grosjean[1,‡], Sascha Dalessi[2,3], Laetitia Basterra[1], Sven Bergmann[2,3], Anne Paoletti[4,5], and Sophie G Martin[1,*]

[1]Department of Fundamental Microbiology; University of Lausanne; Lausanne, Switzerland; [2]Department of Medical Genetics; University of Lausanne; Lausanne, Switzerland; [3]Swiss Institute of Bioinformatics; University of Lausanne; Lausanne, Switzerland; [4]Institut Curie; CNRS UMR144; Paris, France; [5]CNRS UMR144; Paris, France

[†]These authors contributed equally to this work.

[‡]Current affiliation: CSGA; UMR 6265-CNRS; Dijon, France

Keywords: gradient, fission, yeast, *Schizosaccharomyces pombe*, cell cycle, cell growth, cell division, Pom1 DYRK kinase

Where and when cells divide are fundamental questions. In rod-shaped fission yeast cells, the DYRK-family kinase Pom1 is organized in concentration gradients from cell poles and controls cell division timing and positioning. Pom1 gradients restrict to mid-cell the SAD-like kinase Cdr2, which recruits Mid1/Anillin for medial division. Pom1 also delays mitotic commitment through Cdr2, which inhibits Wee1. Here, we describe quantitatively the distributions of cortical Pom1 and Cdr2. These reveal low profile overlap contrasting with previous whole-cell measurements and Cdr2 levels increase with cell elongation, raising the possibility that Pom1 regulates mitotic commitment by controlling Cdr2 medial levels. However, we show that distinct thresholds of Pom1 activity define the timing and positioning of division. Three conditions—a separation-of-function Pom1 allele, partial downregulation of Pom1 activity, and haploinsufficiency in diploid cells—yield cells that divide early, similar to *pom1* deletion, but medially, like wild-type cells. In these cells, Cdr2 is localized correctly at mid-cell. Further, Cdr2 overexpression promotes precocious mitosis only in absence of Pom1. Thus, Pom1 inhibits Cdr2 for mitotic commitment independently of regulating its localization or cortical levels. Indeed, we show Pom1 restricts Cdr2 activity through phosphorylation of a C-terminal self-inhibitory tail. In summary, our results demonstrate that distinct levels in Pom1 gradients delineate a medial Cdr2 domain, for cell division placement, and control its activity, for mitotic commitment.

Introduction

How cell size is controlled and maintained during successive rounds of cell divisions is a question that has long fascinated cell biologists. Cell size is a key feature for the proper organization and function of tissues and organs in multicellular organisms, or for survival and competitive fitness in unicellular microorganisms.[1,2] Cell size control requires the precise coordination of cell growth with cell division. In microorganisms, evidence for such coordination has been known for a long time. In animal cells, analysis of cell size control has been slowed by technical limitations. Recently, however, measurements of growth in human cell lines using microfluidic devices or on fixed steady-state populations with help of mathematical modeling, revealed regulatory events at the G_1/S transition, decreasing cell size variation.[3-5]

In the fission yeast *Schizosaccharomyces pombe,* a rod-shaped single-cell eukaryote that exhibits stereotyped patterns of growth by cell tip extension and division by medial cleavage, direct evidence for cell size control has existed since the 1970s, when it was shown that cells rapidly re-establish their normal length upon recovery from a transient cell cycle block.[6] In this organism, one major homeostatic mechanism operates at the G_2/M transition, when cells can adjust the time spent in G_2 to divide only when a specific cell size has been reached.[7,8] This transition is driven by CDK1, whose activation timing is dictated by the balance between the inhibitory Wee1 kinase and the activating Cdc25 phosphatase.

We and others proposed a cell size-sensing mechanism, where cells geometrically monitor their length to control cell division.[9,10] This relies on the DYRK-family kinase, Pom1, which negatively regulates its substrate, the SAD-like kinase Cdr2. In turn, Cdr2 functions in a negative regulatory cascade to inhibit Wee1.[11,12] Cdr2 assembles into cortical clusters, or nodes, at mid-cell,[13] which contain several additional components, including the Wee1-inhibitory kinase Cdr1/Nim1[14-16] and Wee1 itself.[10,17] By contrast, Pom1 forms concentration gradients from cell poles, associating with the plasma membrane in a phosphorylation-regulated manner.[18] Buffering mechanisms have further been

*Correspondence to: Sophie G Martin; Email: Sophie.Martin@unil.ch
Submitted: 10/29/2013; Revised: 11/29/2013; Accepted: 12/02/2013; Published Online: 12/06/2013
http://dx.doi.org/10.4161/cc.27411

proposed to reduce noise in these gradients.[19] Measurements of Pom1 distribution over the entire cell volume suggested that cell elongation, by driving the gradients' sources at cell poles apart, leads to Pom1 concentration decrease at mid-cell.[9,10] In the proposed model, Pom1 negatively regulates Cdr2 in short cells, preventing mitotic entry until a critical size has been reached. Whether Pom1 strongly serves as length sensor has, however, been put into question by recent data showing that *pom1*Δ cells are able to adjust their length after perturbation.[20]

Intriguingly, Pom1 and Cdr2 not only regulate division timing, but also division site positioning. Here, Cdr2 plays a positive role in defining a medial division plane, as it recruits to the medial cortex Mid1/Anillin, which, in turn, controls the assembly of the contractile ring.[21,22] This pathway works in parallel to a second pathway promoting medial division by coupling division plane position to nuclear position via nuclear shuttling of Mid1[21] (see also refs. 23–25 for reviews). By contrast, Pom1 plays a negative role in division site positioning, preventing division near cell poles. This occurs largely through regulation of Cdr2 localization: in *pom1*Δ cells, which are also defective for bipolar growth, Cdr2 nodes are no longer restricted to mid-cell and invade the non-growing cell tip,[9,10] with the division site bisecting the Cdr2–Mid1 domain.[26,27] Forced localization of Pom1 at the cell middle also disrupts Cdr2 localization.[10] One important question is how these 2 Cdr2-dependent functions of Pom1 in temporal and spatial regulation of division are coordinated.

Here, we make 3 main discoveries: we quantitatively describe the profiles of Pom1 and Cdr2 at the cell cortex, which reveal much lower length-dependent overlap than previously appreciated; we demonstrate that distinct Pom1 levels define the location of Cdr2 node assembly and the timing of their activation; finally, we show that Pom1 inhibits Cdr2 function independently of regulating its localization. Thus, distinct levels in Pom1 gradients serve to localize and inhibit the same substrate to position division and delay mitosis.

Results

Description of Pom1 and Cdr2 cortical distributions over the cell cycle

The regulation of Cdr2 by Pom1 likely takes place at the plasma membrane, where both proteins localize. To describe the distributions of Pom1 and Cdr2 at the plasma membrane over the cell cycle and probe how these proteins may sense cell size, we developed a semi-automated image analysis plug-in (called Cellophane), allowing measurement, sorting, and averaging of cortical profiles for cells of defined cell length (**Fig. 1A and B**; **Fig. S1A–D**, see extended "Experimental Procedures"). These exclude most, but maybe not all, cytoplasmic contributions of Pom1 (see "Discussion" for a possible function of Pom1 in the cytoplasm). The shape of the Pom1 gradient from cell ends remained identical in cells of increasing sizes, with a medial region of basal (but non-zero) amounts of Pom1 that widened linearly with cell length (~3-fold from cell birth to mitotic entry; **Fig. 1B–D**). The constant shape of Pom1 gradients in cells of distinct lengths is in agreement with the idea that it may serve as a measure of cell length. Remarkably, however, the amount of Pom1 at the very cell middle was identical in cells of distinct cell lengths (**Fig. 1E**).

Cdr2 domain width and intensity also increased ~1.5-fold over the cell cycle (**Fig. 1B, D, and F**). Manual analysis of Pom1 and Cdr2 node distributions in wild type or *cdc25-22* mutant, which divides at a longer cell size, confirmed these results (as previously also noted in ref. 13) and further showed a linear increase in node numbers with cell length (as reported recently in ref. 28) (**Fig. 1G**; **Fig. S1E and F**). Thus, Cdr2 domain grows in length, node number, and intensity as cells grow longer within an enlarging region of basal Pom1.

We note that the Pom1 basal domain enlarged faster than the Cdr2 domain (**Fig. 1D**; **Fig. S1F**). Consistently, the degree of overlap between the Pom1 and Cdr2 curves, as measured by the fluorescence value at the intersection of the curves, diminished slowly with cell length (**Fig. 1H**). Thus, both Pom1 and Cdr2 profiles contain information about the length of the cell, and the overlap between the 2 curves is small.

These results contrast with previously published Pom1 distributions derived from sum projections of total cellular fluorescence, including cytoplasm,[9,10] which described significantly higher Pom1 levels, and thus overlap with Cdr2, at the middle of short cells. They raise the question of how Pom1 negatively regulates Cdr2 for mitotic commitment. Two main hypotheses can be formulated: (1) Pom1 may prevent Cdr2 node assembly at cell poles, as for its role in division placement. The widening of the basal-level Pom1 zone would allow for an increase in Cdr2 amounts at the medial cortex, eventually reaching a threshold for mitotic commitment. This model does not require overlap between Pom1 and Cdr2—indeed, it presumes that their localizations be non-overlapping; (2) Pom1 may inhibit Cdr2 activity. We use here the term "Cdr2 activity" not to strictly describe kinase activity, but to convey more widely "Cdr2 functionality", independent of localization. We do not address here directly whether Pom1 serves as length sensor: this inhibition may take place constitutively at the cell middle within the basal Pom1 domain, or in a cell length-dependent manner within the cell length-dependent overlap zones between Pom1 and Cdr2 or even along the entire plasma membrane (see "Discussion"). A combination of both models can also be envisaged. Below, we test some predictions made by these models.

A separation-of-function allele of *pom1* reduces cell size at division without affecting Cdr2 localization

Pom1 is known to regulate Cdr2 localization.[9,10] Thus, a first simple hypothesis, as stated above, is that Pom1 controls mitotic timing through regulating Cdr2 localization.

However, while dissecting the mechanisms of Pom1 gradient formation,[18] we fortuitously identified a novel *pom1* separation-of-function allele, $pom1^{\Delta 305N}$, by integrating at the *pom1* locus under endogenous promoter our longest N-terminal truncation (deletion of aa 10-303) still competent for localization. $pom1^{\Delta 305N}$ cells displayed no defects in septum position and minor defects in switch to bipolar growth. By contrast, these cells divided at a shorter cell size than wild-type cells (**Fig. 2A**). Thus, the functions of Pom1 in temporal and spatial regulation of cell division can be genetically separated.

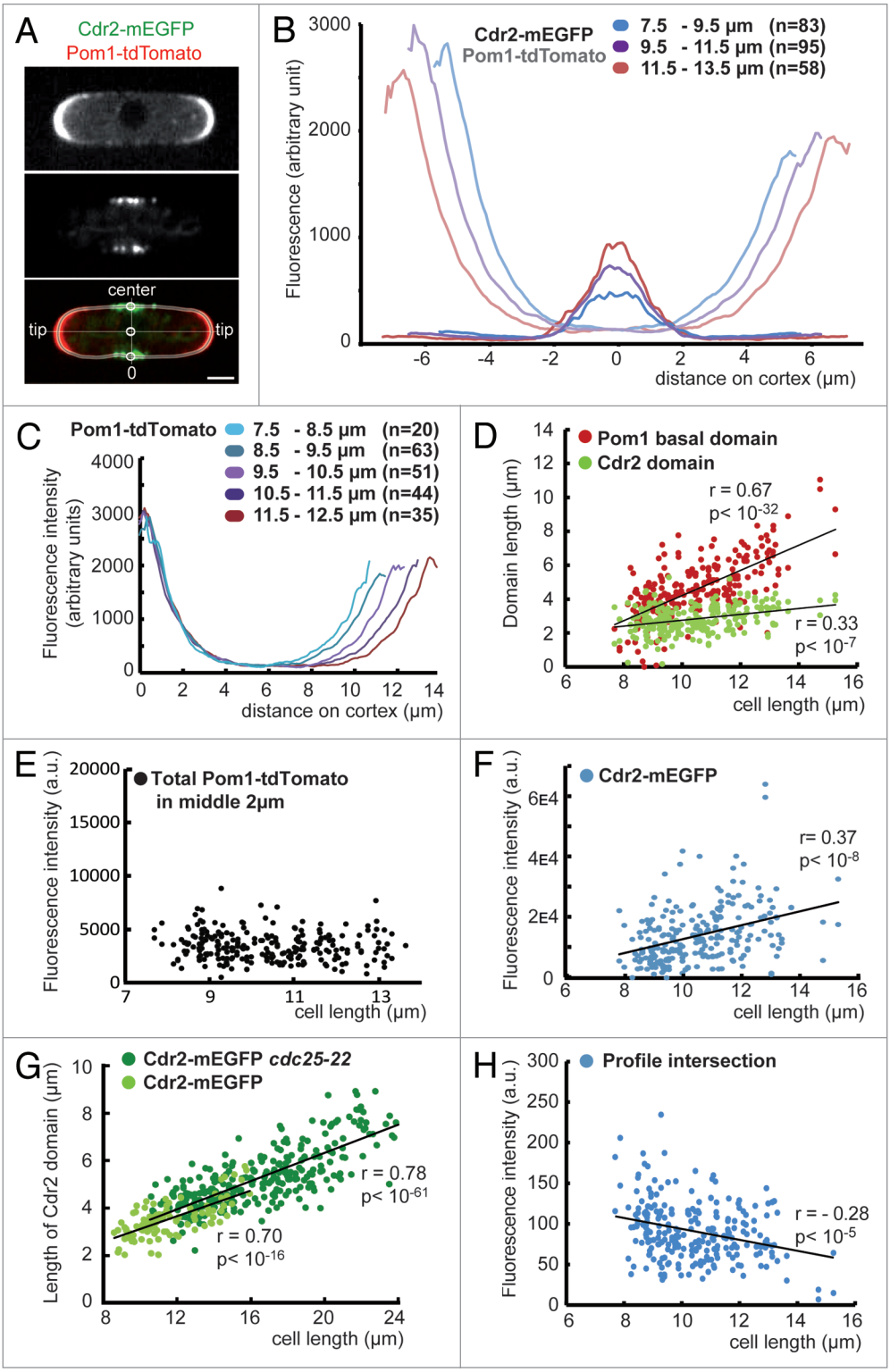

Figure 1. Distribution of Pom1 and Cdr2 in wild-type cells. (**A**) Average projection of 5 middle sections taken at 2-s intervals of Pom1-tdTomato and Cdr2-mEGFP, and segmented cell cortex as obtained from the Cellophane plugin. Landmarks for cell tips and center are used to subsequently align the fluorescent profiles. (**B**) Distribution of Pom1 and Cdr2 at the cortex of wt cells of increasing length, obtained with the Cellophane plugin. By convention the high peak of Pom1 is represented on the left. (**C**) Pom1-tdTomato distribution on the cell cortex in cells of different cell sizes aligned to the tip. (**D**) Length of the Cdr2-mEGFP domain above a threshold of 150 (a.u.) and of the Pom1-tdTomato basal domain below a threshold of 150 (a.u.) relative to cell length in a wt background. (**E**) Total cortical Pom1 level over 2 µm at the cell middle relative to cell length. (**F**) Integrated intensity of the Cdr2-mEGFP signal over a threshold of 150 (a.u.) relative to cell length in wild-type cells. (**G**) Manual measurement of the length of the domain occupied by Cdr2 nodes relative to cell length in wt and *cdc25-22* cells. (**H**) Fluorescence level (a.u) at the points where Pom1-tdTomato and Cdr2-mEGFP profiles intersect. All *P* values are obtained from 2-sided linear regression tests.

We investigated the distribution of Cdr2 in *pom1*$^{\Delta 305N}$ mutant cells: Cdr2 domain width and intensity at the cell middle showed no, or only minor, changes compared to wild-type cells of identical length (**Fig. 2B**), consistent with the normal septum position. Cdr2 node localization is controlled not only by Pom1, but also by an as-yet-undefined, growth-dependent pathway, with Cdr2 spreading all around only the non-growing cell end of *pom1*Δ cells.[9,10] To test whether Cdr2 remained restricted to the cell middle in *pom1*$^{\Delta 305N}$ cells due to their still largely bipolar growth, we investigated the effect of *pom1*$^{\Delta 305N}$ in otherwise monopolar *bud6*Δ cells,[29] in which Pom1 localizes normally (**see Fig. S3A**). Here again, Cdr2 distribution and septum position were unaffected by *pom1*$^{\Delta 305N}$ (**Fig. S2A and B**; septum placement at 0.472 ± 0.018 of cell length in *bud6*Δ vs. 0.475 ± 0.020 in *bud6*Δ *pom1*$^{\Delta 305N}$), indicating that, even in cells growing in a monopolar manner, *pom1*$^{\Delta 305N}$ does not affect Cdr2 localization. Thus, Pom1-dependent regulation of mitotic commitment appears largely independent of Cdr2 localization.

Distinct levels of Pom1 activity regulate division timing and positioning

What is the underlying defect of *pom1*$^{\Delta 305N}$? Pom1$^{\Delta 305N}$-GFP localized at cell tips, formed gradients similar to wild-type Pom1, but was present at about 60% of wild-type levels as assessed by both western blotting and GFP fluorescence quantification (**Fig. 2C–E**). However, both overexpression of *pom1*$^{\Delta 305N}$ under *nmt41* promoter and mis-targeting of Pom1$^{\Delta 305N}$ to the cell middle by fusion with Cdr2 C terminus produced an increase in cell length at division, similar to that observed with full-length Pom1 (**Fig. 2F**; **Fig. S2C and D**),[9] indicating that this allele is still able to delay mitotic entry. Consistently, Pom1$^{\Delta 305N}$ remained fully active in vitro (**Fig. S2E**). Though we cannot exclude that this allele may also be deficient in specific molecular interactions, the lower expression levels of Pom1$^{\Delta 305N}$ and its preserved ability to delay mitotic entry upon overexpression suggest that distinct levels of Pom1 or Pom1 activity may regulate division timing and positioning.

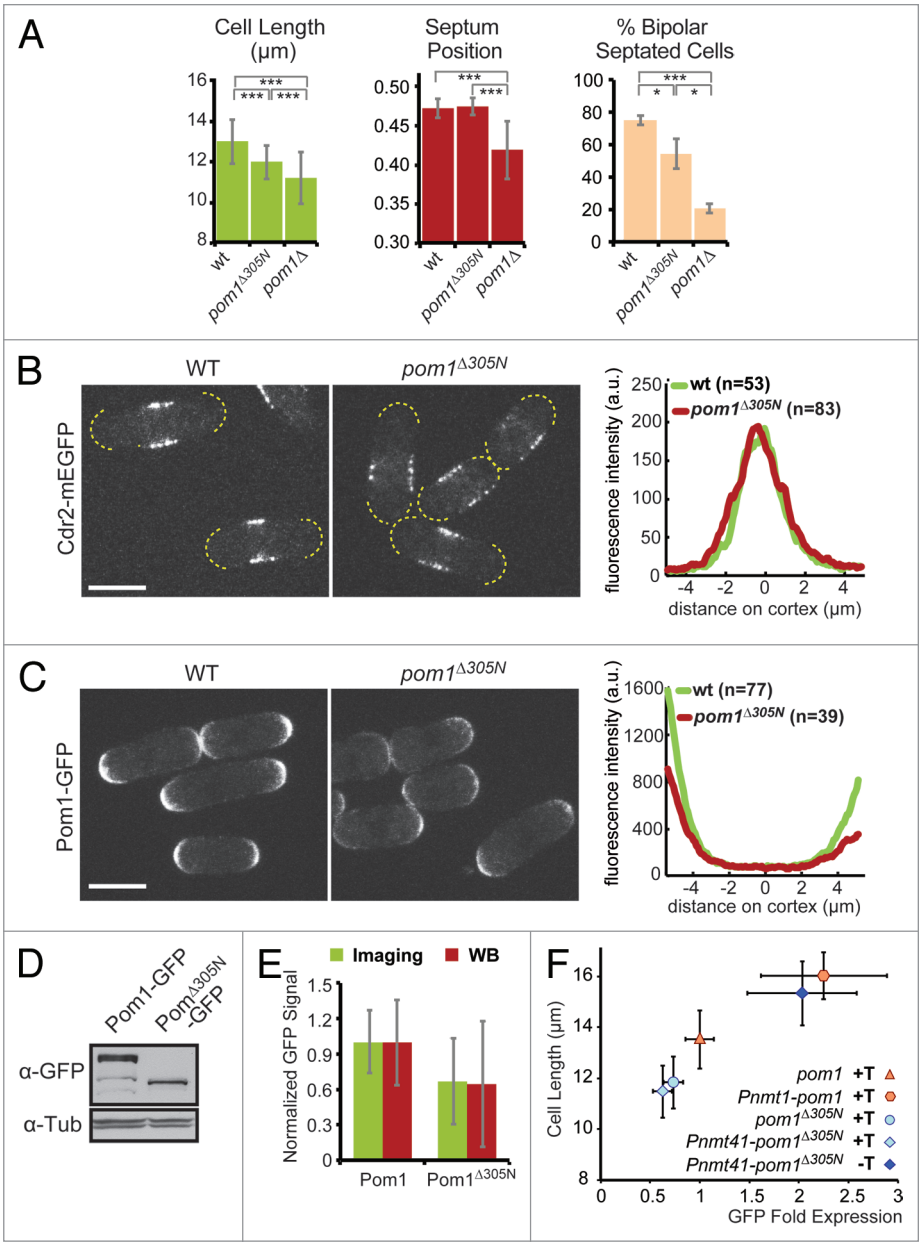

Figure 2. A separation-of-function allele of *pom1* reduces cell size without affecting Cdr2 localization. (**A**) Mean cell length at division (left), mean septum position (middle), and mean % bipolar septated cells (right) in wt, *pom1*$^{\Delta 305N}$ and *pom1*Δ cells (n > 190 for each measure from 3 independent experiments). Error bars: SD. (**B**) Localization of Cdr2-GFP in wt and *pom1*$^{\Delta 305N}$ background, and distribution profiles in 8.5–10.5-μm cells as obtained using Cellophane Plugin (right). Data from one of 3 experiments is shown. Cell tips are outlined. Spinning disk medial plane images. Bar: 5 μm. (**C**) Localization of GFP-tagged Pom1 and Pom1$^{\Delta 305N}$ mutant, and distribution profiles in 8.5–10.5-μm cells as obtained using Cellophane plugin (right). Data from one of 3 experiments is shown. Spinning-disk maximum projections. Bar: 5 μm. (**D**) Western blot of total protein levels of GFP-tagged Pom1 in same strains as in (**C**) Alpha-tubulin serves as the loading control. (**E**) Quantification of the intensity of GFP signals as seen in western blots (corrected to the tubulin signal) and in cells (corrected to background signal and signal from an untagged strain, n = 36 cells), on strains as in (**C**). Values of Pom1-GFP set to 1. Error bars: SD. (**F**) Mean cell length at division and normalized mean intensity during interphase of Pom1-GFP and Pom1$^{\Delta 305N}$-GFP expressed from *pom1* promoter or overexpressed from *pnmt41* or *nmt1* promoter. Cells were grown in EMM+3S for 24 h with or without thiamine. One of 3 experiments is shown. Error bars: SD.

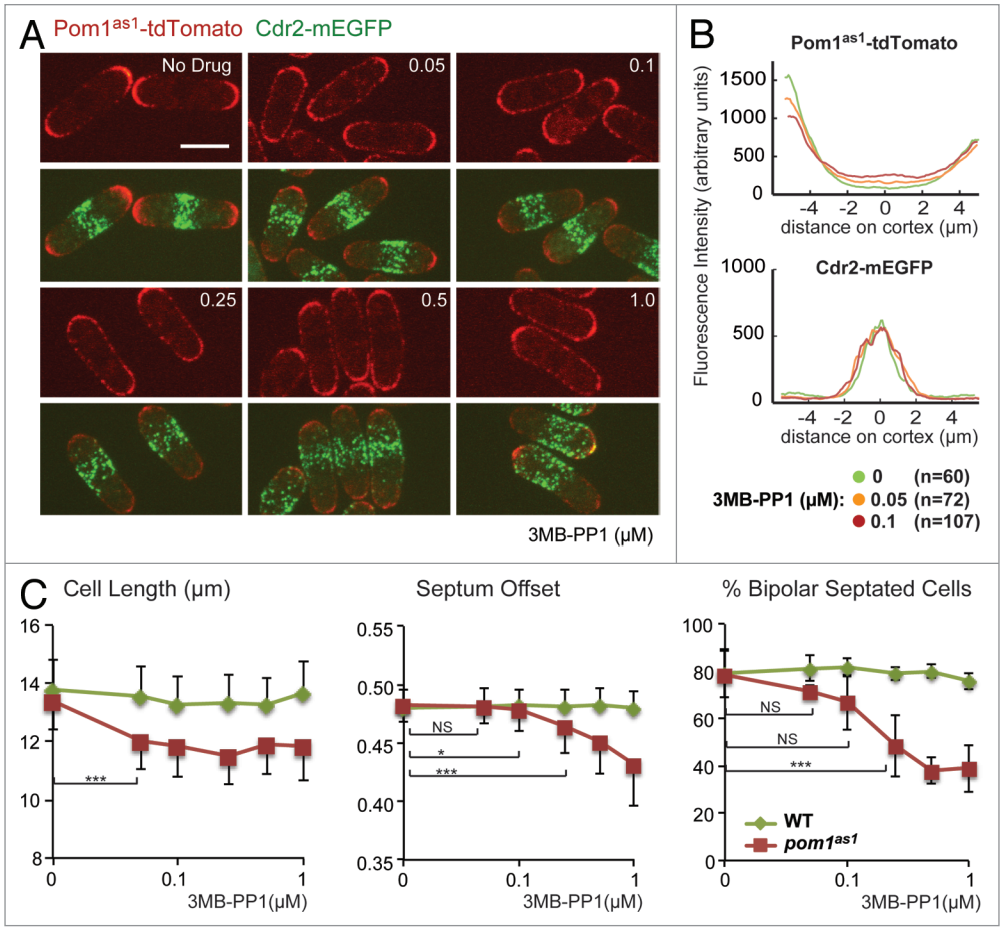

Figure 3. Partial inhibition of Pom1 activity separates its functions in mitotic commitment and Cdr2 localization. (**A**) Localization of Pom1^{as1}-tdTomato (red) and Cdr2-mEGFP (green) with increasing doses of 3MB-PP1. Top panels show medial section confocal images of Pom1^{as1}-tdTomato; bottom panels show maximum projections of the merged channel. Bar: 5 μm. (**B**) Distribution of Pom1^{as1}-tdTomato and Cdr2-mEGFP in 7.5–9.5 μm cells as in (**A**), obtained with the Cellophane plugin. (**C**) Mean cell length at division (left), mean septum position (middle) and mean % bipolar septated cells (right) in wt and *pom1^{as1}* from 3 independent experiments. Error bars: SD.

We tested this hypothesis more directly. First, we used an analog-sensitive allele, Pom1^{as1}, which can be inhibited by small-molecule inhibitors of the PP1 family. We had previously shown that 10–20 μM 1NM-PP1 blocks Pom1^{as1}.[9,27] 3MB-PP1 was about 10-fold more efficient, with 1 μM fully inhibiting Pom1^{as1} or Pom1^{as1}-tdTomato, producing *pom1^{KD}*-like phenotypes, but having no undesired off-target effects on wild-type cells (**Fig. 3A–C**). Like *pom1^{KD}* or *pom1*Δ, these cells showed Pom1 delocalization, NETO failure, Cdr2 domain extension over the non-growing cell half, and division off-center at short cell size (**Fig. 3A–C**).

Remarkably, 10–20-fold lower 3 MB-PP1 dosage (0.05–0.1 μM) separated Pom1 functions, resulting in bipolar cells dividing medially at short cell size, with Cdr2 medial localization and amounts similar to wild-type (**Fig. 3B and C**; **Table S3**). At these low doses, Pom1 was clearly partially inhibited, as it moderately delocalized along the lateral cell cortex (**Fig. 3A and B**; refs. 18 and 30). Intermediate 3MB-PP1 dosages (0.25–0.5 μM) had similarly short cells, with progressively more severe Cdr2 delocalization and division site mispositioning defects (**Fig. 3A and C**). The distribution of Cdr2 was not dependent on the growth pattern of the cells, as it remained unchanged in uniformly monopolar *bud6*Δ cells compared to *bud6*+ cells (**Fig. S3B**). Thus, partial reduction of Pom1 activity by pharmacological inhibition affects cell division timing but not Cdr2 localization or cell division positioning.

Pom1 is haploinsufficient for control of mitotic commitment

To test the importance of Pom1 protein dosage, we used diploid cells, in which, like in haploids, *pom1* deletion led to shorter cell size at division and mispositioned septa (**Fig. 4A and B**). Remarkably, heterozygous *pom1*Δ/*pom1*+ diploid cells were significantly shorter than wild-type cells, but divided medially (**Fig. 4A and B**; **Table S4**). Thus, *pom1* is haploinsufficient for its role in division timing, but not positioning, indicating that here again the 2 functions require distinct levels of Pom1 protein.

We investigated the distribution of Pom1 and Cdr2 in diploid wild-type *pom1-tdTomato*/*pom1-tdTomato* and heterozygous *pom1*Δ/*pom1-tdTomato* cells. In both cases, one copy of Cdr2 was tagged with GFP. As in haploids, Pom1 formed polar gradients and small clusters (**Fig. 4C**).[18,19] In the wild-type cells, Pom1

gradients from cell ends remained of constant shape in cells of distinct lengths, reaching a uniform basal level at the cell middle (**Fig. 4D**), though Cdr2 domain width and levels did not increase with cell length. As in haploid cells, there was an overlap between Pom1 and Cdr2 profiles. However, this overlap was almost constant and diminished only very moderately with cell length (**Fig. 4G**). In heterozygous *pom1Δ/pom1+* diploid cells, Pom1 levels were significantly reduced throughout the cortical profile, including within the medial basal domain (**Fig. 4E and F**). Cdr2 was localized normally at the cell middle, and again its levels did not increase with cell length (**Fig. 4E**). A largely constant overlap was also present at the intersection of both profiles but, probably owing to the lower Pom1 medial levels, was lower than in the wild-type situation (**Fig. 4G**).

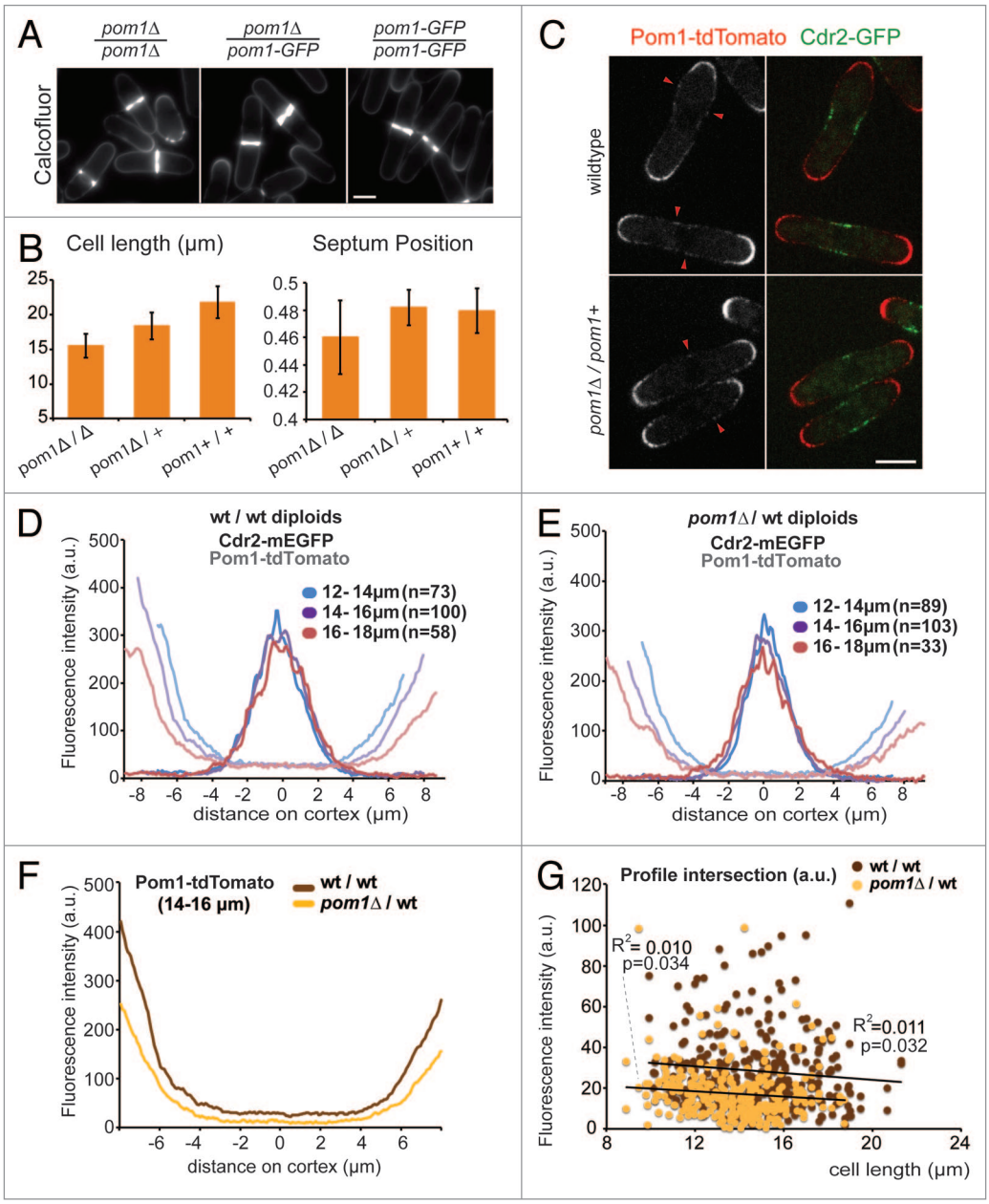

Figure 4. *pom1* is haploinsufficient for mitotic timing. (**A**) Calcofluor staining of *pom1-GFP/pom1-GFP*, *pom1Δ/pom1-GFP*, and *pom1Δ/pom1Δ* diploid cells. (**B**) Mean cell length at division (top), mean septum position (botton) in strains as in (**A**). Error bars: SD. (**C**) Localization of Pom1-tdTomato (grey and red) and Cdr2-mEGFP (green) in wt and heterozygote *pom1Δ/pom1+* diploid cells. In both strains, a single *cdr2* allele was tagged and all *pom1+* alleles were tagged. Red arrowheads highlight a few Pom1 clusters. (**D**) Distribution of Pom1 and Cdr2 at the cortex of wt diploid cells (as in **C**) of increasing length, obtained with the Cellophane plugin. By convention the high peak of Pom1 is represented on the left. (**E**) Distribution of Pom1 and Cdr2 at the cortex of heterozygote *pom1Δ/pom1+* diploid cells (as in **C**) of increasing length, obtained with the Cellophane plugin. By convention the high peak of Pom1 is represented on the left. (**F**) Comparison of the Pom1 profiles in 14–16-μm-long wild-type and *pom1Δ/pom1+* diploid cells, as in (**D and E**). (**G**) Fluorescence level (a.u) at the points where Pom1-tdTomato and Cdr2-mEGFP profiles intersect in both wt and *pom1Δ/pom1+* diploid cells. Note that *P* values were obtained from 1-sided linear regression tests.

In summary, 3 independent lines of evidence demonstrate that partial reduction in Pom1 protein levels or Pom1 activity separates its functions in timing and positioning of cell division: division timing requires higher global Pom1 (activity) levels and is more sensitive to an alteration of these levels.

Pom1 negatively regulates Cdr2 activity

The largely unchanged distributions of Cdr2 in these *pom1* separation-of-function conditions presented above make the model that Pom1 simply controls mitotic entry by modulating Cdr2 increase at the cell middle unlikely. In addition, we

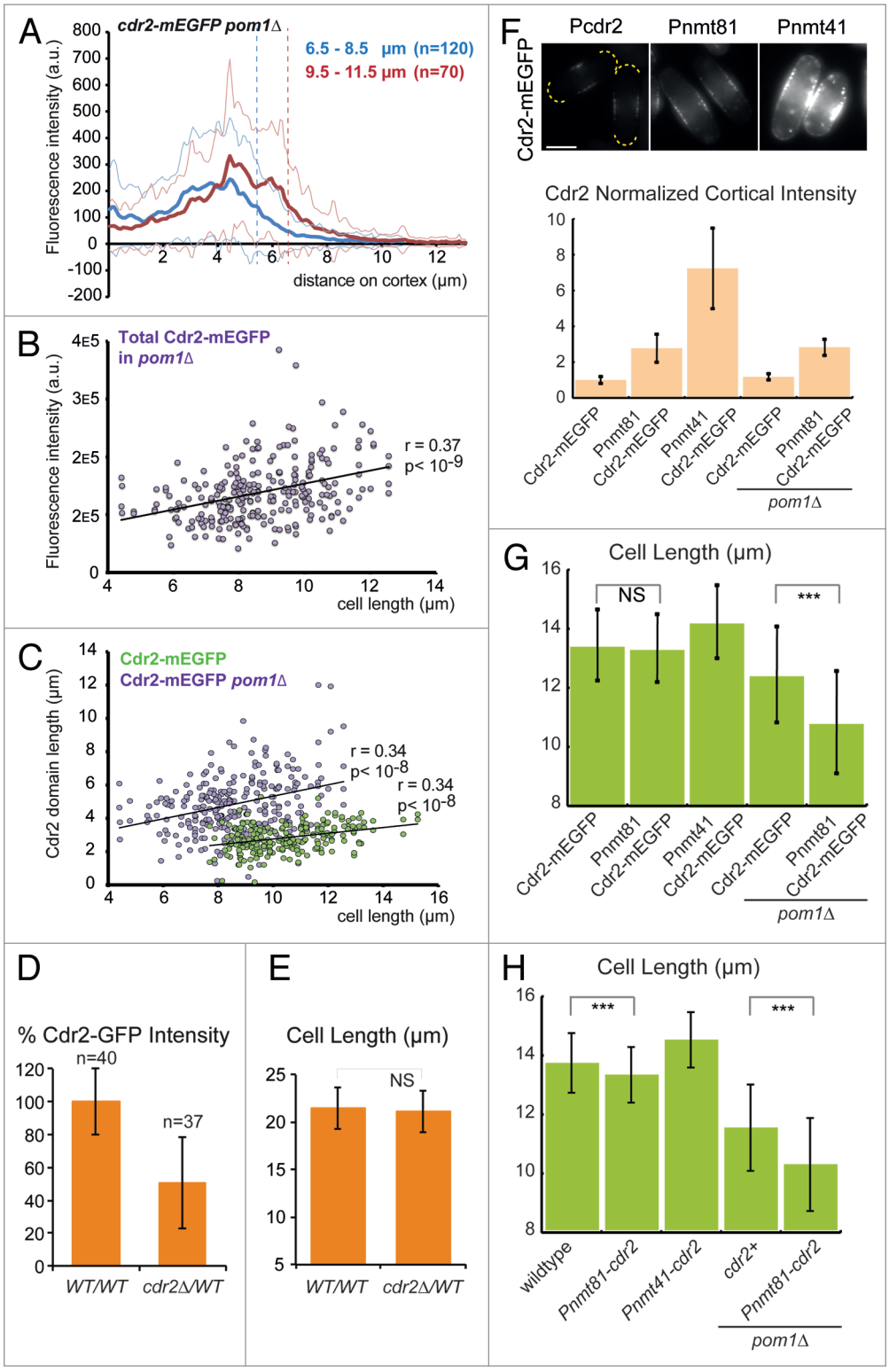

Figure 5. For figure legend, see page 545.

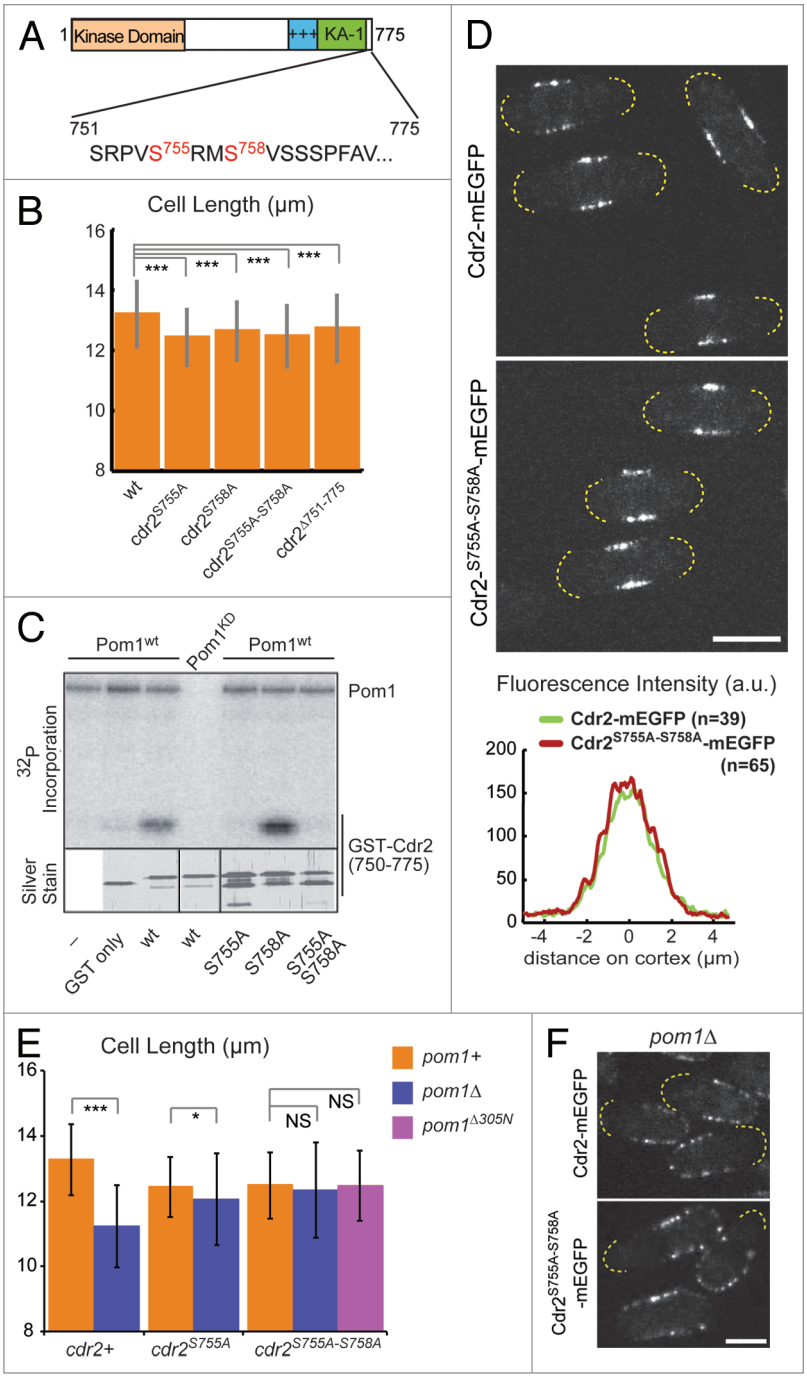

Figure 6. Pom1 negatively regulates Cdr2 through Cdr2 C-terminal tail. (**A**) Scheme of Cdr2, showing the kinase domain, a basic (+++) and KA-1 domain mediating membrane binding and the C-terminal tail, which was either truncated or mutated at indicated positions (red). (**B**) Mean cell length at division in wt and indicated *cdr2* mutants. Error bars: SD. (**C**) In vitro kinase assay of GST-Pom1 on GST-Cdr2$_{750\text{-}775}$ with indicated mutation or on GST alone. The fourth lane is an assay of GST-Pom1^{KD} on GST-Cdr2$_{750\text{-}775}$. Top panel shows phosphorimager detection of ^{32}P incorporation; bottom panel shows silver-stained gel. (**D**) Localization and distribution profiles of Cdr2-mEGFP and Cdr2$^{S755A\text{-}S758A}$-mEGFP in 7.5–9.5-μm cells using automated Cellophane plugin. Data from one of 2 experiments is shown. Cell tips are outlined. Bar: 5 μm. (**E**) Deletion or truncation of *pom1* have no or little effect in *cdr2^{S755A}* and *cdr2$^{S755A\text{-}S758A}$* mutant cells. Mean cell length of indicated genotypes. Error bars: SD. (**F**) Localization of mEGFP-tagged Cdr2 and Cdr2$^{S755A\text{-}S758A}$ in *pom1*Δ cells.

note that the Cdr2 domain also increased in width and levels during cell growth in *pom1*Δ cells. This suggests that the dimensions of this domain at the cell cortex are set largely independently of Pom1 during cell elongation (**Fig. 5A–C**). Consistently, simple statistical analysis of Pom1 and Cdr2 profiles in wild-type haploid cells (see **Fig. 1**) showed that Pom1 and Cdr2 profiles contain non-redundant information about cell length. Indeed both the basal Pom1 domain size and the Cdr2 domain area are significantly associated with cell size, even when removing the effect of the other variable ($P < 2E\text{-}46$ and $P < 3E\text{-}8$). Including the Cdr2 domain area in a linear model of cell size as a function of Pom1 basal domain brings the explained variance from 58% to 63%, suggesting that the Cdr2 profile contains information that is not present in the Pom1 profile. Thus, these data are consistent with the notion that Cdr2 medial levels and Pom1-mediated regulation may contribute distinct information for mitotic commitment.

We tested the effect of Cdr2 levels in 2 ways. We first constructed heterozygous *cdr2-GFP/cdr2*Δ diploids and compared them to cdr2-GFP/cdr2+ cells. In these diploids, total Cdr2 levels were halved

Figure 5 (See previous page). Cdr2 cortical levels increase with cell length independently of *pom1* and are inhibited by Pom1. (**A**) Cdr2-mEGFP cortical distribution in *pom1*Δ in cells of 6.5–8.5 μm (blue) compared to cells of 9.5–11.5 μm (red). Standard deviation is indicated by a thin line. Profiles were aligned to the non-growing cell pole, where Cdr2 accumulates. Dashed vertical lines indicate the cell middles. (**B**) Integrated intensity of the Cdr2-mEGFP signal (a.u.) relative to cell length in *pom1*Δ. (**C**) Length of the mECdr2-GFP domain above a threshold of 150 (a.u.) relative to cell length in *pom1*Δ and wild-type cells. All *P* values are obtained from 2-sided linear regression tests. (**D**) Quantification of the intensity of Cdr2-GFP signals in diploid cells of genotypes *cdr2-GFP/cdr2+* (n = 40) and *cdr2-GFP/cdr2*Δ (n = 37). To account for all Cdr2 copies, the measured values for the wild-type were doubled, because only 1 copy of Cdr2 is tagged in this strain. Values of the wild-type set to 1. Error bars: SD. (**E**) Mean cell length at division in strains as in (**D**). Error bars: SD. (**F**) Images and quantification of Cdr2-mEGFP expressed from its own endogenous promoter, from the *nmt81* promoter and from the *nmt41* promoter. All images were taken with identical settings. The normalized mean cortical intensity of Cdr2-mEGFP during interphase in the strains used in (**G**) is shown at the bottom. N = 90 cells grouped from 7 independent experiments for *wt* cells; n = 40 cells grouped from 2 independent experiments for *pom1*Δ cells. Error bars: SD. (**G**) Mean cell length at division in wt or *pom1*Δ cells expressing Cdr2-mEGFP from *cdr2* promoter or overexpressing it from *nmt81* or *nmt41* promoters (n > 400 cells grouped from 7 independent experiments for *wt* cells; n > 240 cells grouped from 2 independent experiments for *pom1*Δ cells). Error Bars: SD. (**H**) Mean cell length at division in wild-type or *pom1*Δ cells with untagged *cdr2+* expressed from *cdr2* promoter or over-expressed from *nmt81* promoter (n > 600 from 6–8 independent experiments each). Cells were grown for 36 h at 30 °C in EMM + 3S without thiamine. Error Bars: SD.

(**Fig. 5D**). However, the length of these cells was the same as that of wild-type diploids (21.1 ± 2.2 μm vs. 21.5 ± 2.2 μm, respectively; **Fig. 5E**; **Table S4**), suggesting that Cdr2 is not limiting for mitotic commitment.

Second, we overexpressed mEGFP-tagged Cdr2 in haploid cells by placing *cdr2* ORF under the control of *nmt81* or *nmt41* promoters at the *cdr2* endogenous locus (**Fig. 5F and G**; **Table S5**). Previous data had shown that strong Cdr2-GFP overexpression caused dominant-negative effects, lengthening cells at division.[13] Similarly, expression from the *nmt41* promoter, which induced a 7-fold fluorescence increase in Cdr2-mEGFP cortical levels compared to expression from *cdr2* promoter, led to an increased cell length at division. By contrast, Cdr2-mEGFP expression from *nmt81* promoter, which induced a 2.8-fold increase in cortical levels, did not show a dominant-negative effect, but also did not show significant reduction in cell length at division. We confirmed these results by overexpression of non-tagged Cdr2. In this case, expression from the *nmt81* promoter caused a small, though significant, reduction in cell length at division in wild-type cells, suggesting that moderate increase in Cdr2 levels can weakly promote mitotic commitment (**Fig. 5H**). Remarkably, however, this same level of Cdr2-mEGFP or untagged Cdr2 expression led to an important reduction in cell length at division in *pom1*Δ cells (**Fig. 5G and H**; **Table S5**). Thus, mild Cdr2 overexpression accelerates mitotic entry much more potently in absence of Pom1.

Together, these results indicate that a cell length-dependent increase in Cdr2 levels may contribute to cell size measure, but only efficiently upon removal of Pom1-mediated inhibition. Thus, Pom1, in addition to controlling Cdr2 localization to the cell middle, also keeps it in an inactive form.

The C-terminal tail of Cdr2 is required for Pom1-mediated inhibition

Some members of the AMPK superfamily, which includes the SAD-like kinases, to which Cdr2 belongs, are subject to auto-inhibition by their C terminus.[31] To test if Cdr2 was subject to auto-inhibition, we produced a mutant carrying a truncation of the very C-terminal tail ($cdr2^{\Delta 751\text{-}775}$) beyond the KA-1 domain-mediating membrane binding (**Fig. 6A**; Rincon et al., in preparation). This truncation did not affect Cdr2 localization,[13] but promoted cell division at a shorter size than wild-type cells (**Fig. 6B**; **Table S6**), suggesting that Cdr2 C-terminal tail negatively regulates Cdr2 activity.

Cdr2 C-terminal tail was phosphorylated by Pom1 in vitro (**Fig. 6C**). Alanine substitution of S755 but not S758, both within DYRK consensus motifs, blocked phosphorylation, showing that Cdr2 is phosphorylated by Pom1 on S755 in vitro. In vivo, $Cdr2^{S755A\text{-}S758A}$-GFP localized medially with similar amounts to wild-type, and these cells divided medially (**Fig. 6D** and data not shown). By contrast, this double mutant, as well as $cdr2^{S755A}$ single mutant, divided at a shorter size than wild-type cells (**Fig. 6B**; **Table S6**). These similar phenotypes to the C-terminal tail truncation are consistent with the notion that Pom1 phosphorylates this region. We note that the $cdr2^{S758A}$ single mutant was also shorter in vivo, suggesting the Cdr2 C-terminal tail is easily unfolded or may be the target of several kinases. Remarkably, *pom1* deletion or N-terminal truncation ($pom1^{\Delta 305N}$) had very little effect on cell length in $cdr2^{S755A\text{-}S758A}$ or $cdr2^{S755A}$ mutant alleles (**Fig. 6E**; **Table S6**), indicating that these alleles are largely insensitive (epistatic) to Pom1. However, in *pom1*Δ cells, these double mutants showed mis-positioned septa, like *pom1*Δ single mutant. In addition, $Cdr2^{S755A\text{-}S758A}$-GFP, like wild-type Cdr2-GFP, was aberrantly localized around the non-growing cell end (**Fig. 6F**), indicating that this allele remains sensitive to Pom1-dependent localization signal.

In summary, these data are consistent with the idea that Cdr2 C-terminal tail serves to inhibit Cdr2 activity upon phosphorylation by Pom1. Removal of this inhibitory mechanism renders Cdr2 largely insensitive to Pom1-dependent regulation of its functionality for mitotic commitment, but does not affect its localization for division site placement. Thus, 2 distinct Pom1 signals independently regulate Cdr2 activity and localization.

Discussion

Where and when cells divide are important biological questions. In fission yeast, Pom1 kinase is involved in both temporal

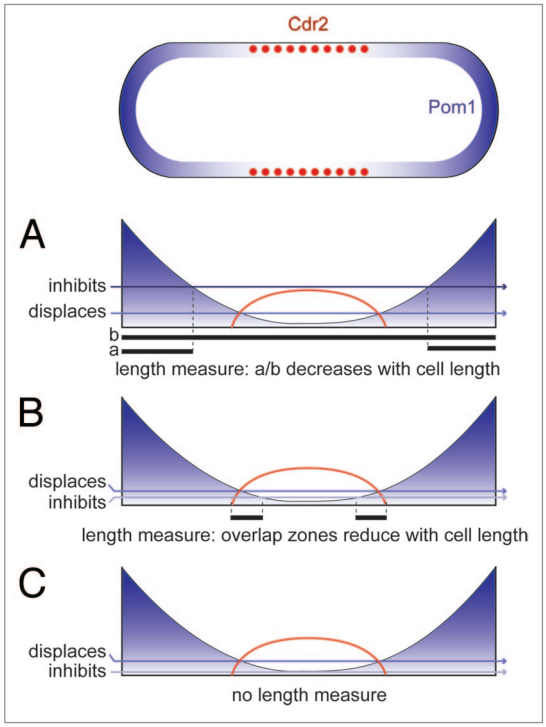

Figure 7. Possible models of differential Pom1-dependent regulation of Cdr2 and cell length sensing. (**A**) Pom1 may inhibit Cdr2 in regions of high Pom1 concentration near cell poles, concomitant with Cdr2 detachment from the plasma membrane, leading to accumulation of inhibited Cdr2 at the cell middle. Cell length may be perceived through the ratio of Pom1-covered to total cell cortex. (**B**) Pom1 may inhibit Cdr2 primarily in the zones of overlap between Cdr2 and Pom1 profiles. Reduction of the extent of overlap with cell length may provide a measure of cell length. (**C**) Pom1 may inhibit Cdr2 throughout the medial domain, and not serve as cell length sensor, though even in this case the cell length-dependent overlap on the edges of the medial domain may modulate this inhibition. In each model, the horizontal lines indicate possible concentration levels at which Pom1 exerts its inhibitory and displacing activities on Cdr2. See text for details.

and spatial regulation of cell division. We and others have previously shown that Pom1 is an inhibitor of mitotic commitment, which negatively regulates Cdr2, itself part of a Wee1 inhibitory pathway.[9,10] These studies proposed that the polar Pom1 gradients form a size-perception system to couple cell length with mitotic entry, though recent data challenged the view that Pom1 acts as cell length sensor.[20] Pom1 also ensures medial placement of the division plane by restricting Cdr2 and Mid1/anillin node localization to the medial cortex.[21,26,27] In this study, we provide 3 new lines of evidence that illuminate the interaction between Pom1 and Cdr2. First, we provide a quantitative description of Pom1 and Cdr2 distribution at the cell cortex, which puts in question simple models of cell-length sensing. Second, we show that Pom1 controls mitotic commitment through Cdr2 in ways distinct from the regulation of Cdr2 localization. Finally, we demonstrate that Pom1's function in the timing and positioning of division are genetically separable and mediated by distinct Pom1 levels. Thus, 2 distinct Pom1 levels exert distinct effects on the same substrate for timing and positioning of division.

Two distinct Pom1 signals regulate timing and positioning of division

For division positioning, it has been clearly demonstrated that Pom1 modulates Cdr2 localization.[9,10] Cdr2, in turn, contributes to positioning cell division medially, by localizing Mid1/anillin to the cell middle.[21,26,27] How Pom1 regulates Cdr2 for mitotic commitment has remained an important question. We show here that Pom1 modulates mitotic commitment in ways distinct from its regulation of Cdr2 localization.

Indeed, 4 distinct modifications of Pom1 or Cdr2 function: (1) truncation of the first 300 residues of Pom1 in the *pom1*$^{\Delta 305N}$ allele; (2) partial pharmacological inhibition of Pom1^{as1}; (3) *pom1* haploinsufficiency in diploid cells; and (4) *cdr2* C-terminal tail mutation or truncation, advance the cell cycle without altering Cdr2 distribution patterns at the cell middle. In each case, the cells divide prematurely at a short cell size but localize Cdr2 correctly and divide medially even in cells growing only from one cell pole. Thus Pom1-dependent regulation of mitotic commitment occurs independently of a change in Cdr2 distribution.

Roles of Cdr2 levels and distribution for mitotic timing

Our profile measurements show that, in haploid cells, Cdr2 medial levels and domain width increase with cell length, raising the possibility that Cdr2 medial levels may be important for mitotic commitment. This increase over the cell cycle is largely *pom1*-independent, as it is also observed in *pom1*Δ mutant. In diploid cells, Cdr2 did not significantly increase with cell length. One possibility is that Cdr2 medial levels are defined primarily through a "growth"-dependent pathway that excludes Cdr2 from sites of growth near cell tips. In diploid cells, growth zones may be distant enough from the cell middle, and thus not interfere with Cdr2 levels in cells of any size. In any case, halving Cdr2 levels in diploids had no influence on the timing of mitotic entry. In addition, low-level overexpression of Cdr2 advanced the cell cycle only weakly in wild-type cells, suggesting that, by themselves, Cdr2 levels are a poor indicator of mitotic entry.

Furthermore, it is remarkable that the Cdr2 tail mutants divide at almost the same length in *pom1*+ cells, in which Cdr2 is medially localized, and in *pom1*Δ cells, where Cdr2 covers over half of the cell surface. Therefore, the precise spatial distribution of Cdr2 at the cortex is by itself not a major determinant of cell length control, though it may underlie the remaining length difference observed. In conjunction with Pom1-dependent regulation, Cdr2 localization and amounts may dictate where it encounters regulation by Pom1 and, thus, contribute to the timing of mitotic entry.

In summary, these data are inconsistent with the idea that Pom1 simply controls Cdr2 medial accumulation for mitotic commitment, even if this was implemented in 2 theoretical papers of cell cycle control.[32,33] Instead, they suggest that Cdr2 levels may play a minor role in mitotic commitment timing, but additively or synergistically to relief of Pom1 inhibition.

Pom1 inhibits Cdr2 through its C-terminal tail

If Pom1 does not control mitotic commitment by simply modulating Cdr2 distribution at the cortex, what is the mechanism? We suggest that Pom1 directly inhibits Cdr2 activity or functionality within the medial nodes. This idea is in agreement with the fact that an artificial increase of Cdr2 cortical pool advances mitosis potently only when cells are deleted for *pom1*, suggesting Cdr2 is kept in check by Pom1. We have deciphered a first molecular mechanism for this inhibition. This relies on the phosphorylation by Pom1 of Cdr2 C-terminal tail that may fulfill an auto-inhibitory function when phosphorylated. *cdr2* tail mutants are epistatic to *pom1*, indicating that this represents a major mechanism by which Cdr2 is inhibited by Pom1. Thus, Pom1 inhibits Cdr2 through its C-terminal tail.

Auto-inhibition is classically achieved by intramolecular interactions, as has been documented for some members of the AMPK superfamily of kinase to which Cdr2 belongs, such as MELK1.[31] However, we have not found evidence for intramolecular interactions in Cdr2 (our unpublished results). Further analysis will be necessary to determine whether the Cdr2 tail inhibits Cdr2 kinase activity directly or via other means, such as modulation of interactions with partners involved in cell size control. As the *cdr2* tail mutants divide at a longer cell size than *pom1*Δ cells, Pom1 may also negatively regulate mitotic entry through additional mechanisms, which remain to be characterized. Pom1 may, for instance, phosphorylate other components of the Cdr2 nodes, modulating their accessibility to Cdr2. However, as double mutants between *cdr2* tail mutants and *pom1*Δ are also longer than *pom1*Δ, an alternative explanation is that this Cdr2 C-terminal tail also plays a positive role in Cdr2 activation, which is blocked by these mutations.

The importance of Pom1 levels

All 3 instances of separation of Pom1 functions, where Pom1 is functional to position division medially, but not to delay mitotic entry, correspond to a reduction in Pom1 protein or activity levels. First, in the case of *pom1*$^{\Delta 305N}$, the major identified difference is that this allele is found at about 60% of wt Pom1 levels. However, we cannot exclude that this Pom1 truncation does not cause other adverse effects on Pom1 function. Second, an inhibitor dosage about 20-fold lower than that required for complete inhibition of Pom1 was sufficient to block mitotic control in *pom1*^{as1} cells, suggesting that the control of mitotic entry

is exquisitely sensitive to Pom1 activity levels. We note that in this case Pom1 localization is modified, because Pom1 activity is required for Pom1 detachment from the plasma membrane.[18] The increased amount of Pom1^{as1} at mid-cell upon partial inhibition likely represents inactive Pom1. Finally, the clearest demonstration lies in the diploid experiment, where halving Pom1 levels is enough to accelerate the cell cycle, but does not impede medial division. We conclude that control of mitotic entry requires higher global levels of Pom1 activity than control of division positioning.

There is increasing evidence that several kinases act not as on-or-off switches, but rather exert distinct actions at distinct dosages. For instance, different levels of activity of cyclin-dependent kinase elicit entry into S phase and into mitosis.[34] Similarly, distinct levels of Polo-like kinase are required for mitosis and cytokinesis,[35] and different levels of Aurora kinase underlie its functions in chromosome compaction and in regulation of kinetochore–microtubule interaction.[36] It is also interesting to note that the Pom1-related kinase DYRK1A, which lies within the critical region of human chromosome 21 involved in trisomy, is highly dosage-sensitive, exhibiting both haploinsufficiency and duplication phenotypes in brain growth, though its mode of action appears distinct from that of Pom1.[37,38]

In addition to Pom1-dependent signals, the Cdr2 regulatory network also integrates other inputs. The cell length-dependent increase of Cdr2 cortical levels may contribute in conjunction with Pom1-dependent regulation. Additional regulations are operated at the level of Cdr1 by Nif1, which localizes to cell poles,[9,39] and by Skb1, which localizes to distinct cortical nodes.[28] Finally, a recent study revealed that this network is subject to upstream regulations by the Nek/NIMA-family kinase Fin1, which localizes to the spindle pole body.[40] Future work should determine the relative contribution of each of these inputs for mitotic timing.

Where does Pom1 inhibit Cdr2?

Pom1 and Cdr2 both localize at the plasma membrane, suggesting this is where regulation of Cdr2 by Pom1 takes place. In support of this hypothesis, Cdr2 requires membrane binding to be functional,[13] and forced localization of Pom1 at the medial cortex strongly delays mitotic commitment.[9,10] However, the cytosolic pool of Pom1 may also regulate Cdr2. Indeed, previous data showed that cytosolic Pom1 in *tea4*Δ cells, in which Pom1 is not dephosphorylated and fails to bind the plasma membrane,[18] is still competent to delay the cell cycle, though less potently than membrane-targeted Pom1.[9] This cytosolic pool is very low in wild-type cells, and it is unclear how much it may contribute to Cdr2 regulation. In this work, we focused on the membrane-localized pools of Pom1 and Cdr2.

Our quantifications of Pom1 and Cdr2 profiles at the cell periphery depart from previously published quantifications, which included the entire cell volume including cytoplasm. In these earlier quantifications, Pom1 levels at the cell middle diminished with increasing cell length.[9,10] These previously observed cell length-dependent changes in medial Pom1 levels may be due to cytoplasmic modulations or to cell size-dependent changes in the volume of the nucleus, from which Pom1 is excluded.[41] We now show that Pom1 levels are identical at the medial cortex of short and long cells, though the amounts of Pom1 on the edges of the Cdr2 domain are higher in smaller cells. As discussed above, for mitotic timing Pom1 inhibits Cdr2 in addition to regulating its localization. This thus begs the question of where this inhibition takes place, and whether this occurs in a cell length-dependent manner.

We can consider 3 possible locations of the Pom1-mediated Cdr2 inhibition (**Fig. 7**). In each case, we hypothesize that Cdr2 transiently binds the cortex at random locations, but high concentration of Pom1 near cell poles induces faster detachment, leading to Cdr2 accumulation at mid-cell (Rincon et al., in preparation).

The first model (**Fig. 7A**) is that Pom1 inhibits Cdr2 activity wherever it encounters it around the entire cell cortex, independent of the modulation of cortical dynamics. The observed differential sensitivities to Pom1 levels suggest that Cdr2 inhibitory phosphorylation sites are poorer substrates than sites modulating localization. Inhibition would thus occur mostly close to cell poles where Pom1 concentration is highest. This model does not require an extensive overlap between Pom1 and Cdr2, but would require a slow turnover of Pom1-dependent inhibitory phosphorylation compared to the modifications regulating Cdr2 dynamics on the cortex to allow accumulation of inhibited Cdr2 at the cell middle. This model may accommodate Pom1 as cell length sensor: as cells elongate, the ratio of Pom1-covered to total cortex diminishes, which may reduce the likelihood of Cdr2 inhibition by Pom1. Thus, cell length may be perceived through the ratio of polar to total cortex.

The second model (**Fig. 7B**) is conceptually similar to the original model, with Pom1 inhibiting Cdr2 activity on the edges of its domain, where Cdr2 exposure to Pom1 diminishes as cells elongate. This could trigger mitotic entry in a cell size-dependent manner as originally proposed.[9,10] In this model, the sites modulating Cdr2 activity would be better Pom1 substrates than those modulating Cdr2 dynamics on the cortex. Yet, the low concentration of Pom1 in the regions where it inhibits Cdr2 (at the edges of the Cdr2 domain) would render Cdr2 function in mitotic commitment more sensitive to global modifications of Pom1 activity than Cdr2 localization. The overall small variation in Cdr2 exposure to Pom1 as cells elongate suggests this measurement would be noisy. In addition, the Pom1 and Cdr2 overlap in diploid cells is very poorly correlated to cell length, suggesting this mechanism would not permit size measurements in diploids.

The third possibility (**Fig. 7C**) is that, as above, Pom1 concentration at mid-cell may be too low to displace Cdr2, yet sufficient to inhibit its functionality, but that this inhibition takes place throughout the Cdr2 domain and is not significantly alleviated as cells elongate. In this case, Pom1 gradients would not directly measure cell length, but serve to keep Pom1 away from mid-cell. The uniform medial Pom1 basal levels, in which a cytoplasmic signal could also contribute, would simply function as constitutive buffer for mitotic commitment. Medial cortical levels may be modulated, not as function of cell length, but in response to other stimuli, for instance for cell length adaption under stress. Such a model would be consistent with the recent finding that

*pom1*Δ cells are still homeostatic for cell length control.[20] Future work, for instance through development of tools allowing the distinction of active and inactive Cdr2 in situ, will be required to distinguish between these models.

In summary, our work demonstrates that different levels of the same kinase, organized in concentration gradients, both delineate a functional domain and regulate its activity. One major challenge will be to define how this benefits cell size control.

Materials and Methods

Strain construction and culture

Standard *S. pombe* media and genetic manipulations were used.[42] All strains used in the study were isogenic to wild-type 972 and are described in **Table S1**. Strains from genetic crosses were selected by random spore germination or tetrad dissection and replicated in plates with appropriate supplements or drugs. Transformations were performed using the lithium acetate-DMSO method as described.[43] Standard molecular biology techniques were used to create all plasmids described in **Table S2**.

All *pom1* and *cdr2* mutant alleles were integrated at their respective endogenous locus, as detailed in **Table S1** and below. For generation of $pom1^{\Delta 305N}$ mutant, a DNA fragment linking pom1 5'UTR (725 bp upstream of start of *pom1* ORF) with pom1 ORF (from 910 bp downstream of the start of the *pom1* ORF+569 bp of the 3'UTR) lacking the sequence encoding aa 10-303 was generated by PCR stitching and transformed in a *pom1::ura4+* strain for integration at *pom1* locus in replacement of *ura4* sequence by homologous recombination. Note that the name *Δ305N* is not a direct description of the exact amino acids absent in this allele. Transformants were selected on 5-FOA plates and confirmed by diagnostic PCRs and sequencing. Tagging of $pom1^{\Delta 305N}$ with Cdr2C-GFP was performed as described.[9] Integration of *nmt41* promoter and tagging with GFP were done using a PCR-based approach[43] and confirmed by PCR.

cdr2 phosphosite mutants were produced by site-directed mutagenesis of pSM788, a pBluescript plasmid carrying Cdr2 ORF, 5'UTR and 3'UTR regions between NotI and SalI. Plasmids were digested with NotI and SalI before transformation of YSM1164 for integration at *cdr2* locus in replacement of *ura4* sequence by homologous recombination. Transformants were selected on 5-FOA plates and confirmed by diagnostic PCRs and sequencing. Deletion strains were constructed using a PCR-based approach[43] and confirmed by PCR. $cdr2^{S755A\text{-}S758A}$ was C-terminally tagged with mEGFP by transforming it with NotI-BamHI-AgeI digested fragment of pSM990. Transformants were selected on YE-G418 plates and confirmed by diagnostic PCRs.

To produce the *Pnmt41-cdr2-mEGFP* and *Pnmt81-cdr2-mEGFP* strains, *nmt41* or *nmt81* promoters were inserted at BamHI site in pSR34, a pFA6a-mEGFP-KanMX6 derived plasmid carrying *cdr2* promoter and terminator for integration at *cdr2* locus in replacement of the NatMX6 cassette by homologous recombination. Plasmids were digested with NotI before transformation. For *Pnmt81-cdr2* and $Pnmt81\text{-}cdr2^{S755A\text{-}S758A}$, *nmt81* promoter was inserted at BamHI site in pSR34. Plasmids were digested with NotI, AfeI, and AscI, and the largest band purified before transformation of YSM2224 and YSM2226, respectively.

Diploid strains were created by crossing parental haploids bearing ade-M210 and ade-M216 alleles and selecting diploids on plates lacking adenine (EMM supplemented with uracil and leucine) at 30 degrees. Single colonies were picked on YE plates and imaging was done in EMM supplemented with adenine, uracil, and leucine at 30 °C.

To induce Cdr2 or Cdr2-mEGFP overexpression from *nmt81* and *nmt41* promoters,[44] cells were first grown overnight at 30 °C in EMM supplemented with adenine, uracil, leucine, and thiamine (5 μg/ml) then washed 5 times with sterile water and incubated for 24 h at 30 °C in the same medium without thiamine to induce expression. For Pom1-GFP and $Pom1^{\Delta 305N}$-GFP overexpression from *nmt1* and *nmt41* promoters, cells were grown for 24 h at 30 °C in EMM supplemented with adenine, uracil, leucine, with or without thiamine (5 μg/ml).

For $pom1^{as1}$ mutants, cells were grown overnight at 30 °C in EMM supplemented with adenine, uracil, leucine, diluted in the same medium next morning and required dosages of 3MB-PP1 (Toronto Research Chemicals Inc) dissolved in methanol) were added at O.D»0.4 for 4 h before imaging.

Calcofluor (Sigma) was added at a final concentration of 5 μg/ml from a 200× stock solution (1 mg/ml).

Microscopy and image analysis

For all images shown and analyzed, except those of **Figures 1G and 5F** and **Figures S1E and F**, as well as all images for Cellophane analysis (see below), cells were grown in EMM with appropriate supplements at 30 °C and imaged at room temperature (about 23 °C). Image acquisition was performed on a Perkin Elmer Leica DMI4000B inverted microscope equipped with an HCX PL APO × 100/1.46NA oil objective and a PerkinElmer Volocity Confocal system spinning disk microscope including a Yokagawa CSU22 real-time confocal scanning head, solid-state laser lines and a cooled 14-bit frame transfer EMCCD C9100-50 camera, as described.[45] For Pom1 and Cdr2 signal quantifications with Cellophane, 5 pictures for each channel were acquired over 30 s (1 s exposure time, binning 1).

Images for **Figures 1G and 5F** and **Figure S1E and F** were acquired as follows: Images for **Figures 1G and 5F** and **Figure S1E** were taken on a DMRXA2 upright microscope (Leica Microsystems), equipped with a 100×/1.4NA oil immersion PlanApo objective and a Coolsnap HQ CCD camera (Photometrics), exposure time: 2 s. Images for **Figure S1F** were acquired on a full motorized inverted microscope Nikon Eclipse Ti-E microscope equipped with the Perfect Focus System to maintain the focus, a 100×/1.45-NA PlanApo oil immersion objective, a Mad City Lab piezo stage, a Yokogawa CSUX1 confocal unit a Photometrics HQ2 CCD camera and a laser bench (Errol) with 491-561 nm diode laser, 100 mW each (Cobolt), exposure time for GFP, mCherry, or tdTomato: 2s (or 0.5 s for **Fig. S4B**). Laser power 30% (back pupil of the objective: 1.9 mW), binning 2, electronic gain 3.

For **Figure 5F**, Cdr2-mEGFP cortical fluorescence intensity was measured along the entire cortex of interphase cells with the Linescan tool of Metamorph software (3 pixels width) on single

medial focal planes. The graph represents the mean intensity of ≥60 cells.

Total fluorescence intensity quantifications shown in **Figure 2E** were performed on a sum projection of spinning disk confocal z-stacks of an individual cell. For measurement of total fluorescence intensity, the polygon tool in ImageJ was used to draw a line by hand around the cell and the average fluorescence intensity within the cell was obtained using the Analyze < Measure tool. The fluorescence intensity measured was corrected for both the background fluorescence intensity (measured just outside the cell examined) and the fluorescence intensity of an untagged cell (acquired and measured for fluorescence intensity in the same way as mentioned above).

For quantification of western blots in **Figure 2D**, 50 µg whole-cell lysates were loaded on SDS-PAGE and detected by Western blotting with α-GFP mAb (1/5000, Roche) and α-tubulin mAb (1/10000, kind gift from Andrea Baines). Bands were selected and quantified using the Analyze < Gels < Plot-lanes tool of ImageJ. For each strain, a total of 6 lanes were quantified from 2 independent experiments. The intensity of the α-GFP signal was normalized to that of α-tubulin before setting the Pom1-GFP signal value to 1.

For cell length measurements, cells were grown at 30 °C in EMM supplemented with uracil, adenine, and leucine. Cell length measurements were made with Metamorph software on DIC images of septating cells taken on the DMRXA2 microscope described above (for **Fig. 5G**) or on calcofluor-stained cells imaged with a DeltaVision setup (for all other measurements), as described.[46] In all comparisons made, strains with identical auxotrophies were used.

Image analysis by Cellophane and data processing

Cellophane is an ImageJ plugin we developed for the quantification of a fluorescent signal at the cell cortex. In the manual mode, the user manually traces the cortex using the ImageJ tools. In the automatic mode, fluorescent dextran (Alexa Fluor® 647 at 0.2 µg final concentration; Invitrogen) is added to the medium before imaging and the cell boundaries are automatically extracted using edge detection and a snake algorithm.[47] This provides a higher throughput but a somewhat lower precision. In this study, we have used the manual mode throughout, except for **Figure 2B and C**. In addition to the fluorescent signal at the cell cortex, the plugin also measures the mean cytoplasmic and background signals along with their variance, as well as the cell length. Those values are printed to a file that can be used for further analyses such as profile alignment and averaging. Cellophane is open-source and freely available under a GPL licence (http://www.unil.ch/cbg).

Data were aligned and further analyzed using the R software (http://www.r-project.org/). As Pom1 gradients are often asymmetric at the 2 cell ends, we kept this asymmetry, systematically orienting the profiles with the higher Pom1 intensity peak on the left on all alignments involving Pom1. Cells were pooled in bins 2 µm in length, except for **Figure 1C**, for which 1-µm bins were used. Qualitatively similar results were obtained for both bin sizes. In all comparison of Cdr2 profiles between wild-type and mutant backgrounds, a single bin is shown (**Figs. 2B, 3B, and 6D**). Bins of other cell sizes showed qualitatively similar results (similar profiles in wild-type and mutant backgrounds).

To extract Pom1-tdTomato basal domain length, we used a threshold below which the length of the domain was measured (150 for **Fig. 1**; 80 for **Fig. 4**). To extract Cdr2-mEGFP domain length and intensity we used a threshold above which the length and intensity of the domain were measured (150 for **Fig. 1 and 5**; 40 for **Fig. 4**). The distinct thresholds used were due to distinct fluorescent values of the images. To measure Cdr2 levels in *pom1*Δ (**Fig. 5B**), we did not use a threshold, because this skewed the data due to the significantly wider spread of Cdr2 in *pom1*Δ cells. For the overlap analysis, the mean between the 2 fluorescence values at the intersection of the Pom1-tdTomato and Cdr2-mEGFP curves after smoothing with a Gaussian filter was plotted. Qualitatively similar, but noisier results were obtained when smoothing was omitted (data not shown).

Statistical analysis

For pairwise comparison of average cell length, the Student *t* test was used. Throughout all figures, significance of this statistical test is marked with asterisks, with * indicating $P < 0.05$, ** $P < 10^{-5}$ and *** $P < 10^{-10}$. NS, not significant.

Two-sided linear regression tests were performed to assess the effect of cell length on Pom1 and Cdr2 domain lengths and intensities, except in **Figure 4G**, where one-sided linear regression tests were used. Significant *P* values (all are below 10^{-5}) indicate that the null hypotheses that cell length has no effect on Pom1, or Cdr2 domain lengths can be rejected. Thus, Pom1 and Cdr2 distributions vary with cell length. The corresponding correlation values are denoted by r.

In order to assess the redundancy of the information contained in the Pom1 and Cdr2 profiles, we used an additive linear model including the lengths of the Pom1 basal domain x_p and area of the Cdr2 domain x_c for the cell length y_c : $y_c = a_0 + a_1 x_p + a_2 x_c + \varepsilon$, where ε is the Gaussian noise. Significant *P* values for the linear regression tests on coefficients a_1 and a_2 allow the rejection of the null hypothesis that one profile does not provide information on cell length in addition to the other profile, suggesting that they both contribute additive information

Biochemistry

For bacterial expression and recombinant protein production for kinase assays, Cdr2 fragments amplified from pSM788 or the mutant plasmids were cloned between BamHI and XhoI sites in pGEX-4T-1.

For kinase assays, recombinant Pom1 or Pom1$^{\Delta 305}$ and Cdr2 fragments were obtained as described.[18] Kinase assays were performed in 30 mM Tris pH 8, 100 mM NaCl, 10 mM MgCl2, 1 mM EGTA, 10% glycerol, 1 mM DTT, 20 µM ATP, and 2 µCi [^{32}P] ATP (PerkinElmer) in a 15 µl final volume reaction. After a 30-min incubation at 30 °C, the reaction was stopped by boiling in sample buffer and analyzed by SDS–PAGE. ^{32}P-incorporation was detected in a phosphorimager. Silver staining was done according to the manufacturer's protocol (Pierce® Silver stain kit) to check for equivalent amounts of substrates.

Disclosure of Potential Conflicts of Interest

No potential conflicts of interest were disclosed.

Acknowledgements

We thank A Sansaloni for help with strain construction, J Ahringer, and I Hagan for advice and suggestion, and R Benton for critical reading of the manuscript.

This work was supported by an ERC Starting grant (260493) and a Swiss National Science Foundation research grant (31003A_138177) to SGM and the Ligue Nationale Contre le Cancer (Programme Labellisation and Ile de France), and Mairie de Paris (Programme Emergence) to AP. AP is a member of Labex CelTisPhyBio. SAR received post-doctoral fellowships from Fundacion Ramon Areces and Marie Curie FP7 program. MG-V received a PhD fellowship from Université Paris-Sud.

Supplemental Materials

Supplemental materials may be found here:
www.landesbioscience.com/journals/cc/article/27411

References

1. Jorgensen P, Tyers M. How cells coordinate growth and division. Curr Biol 2004; 14:R1014-27; PMID:15589139; http://dx.doi.org/10.1016/j.cub.2004.11.027
2. Mitchison JM. Growth during the cell cycle. Int Rev Cytol 2003; 226:165-258; PMID:12921238; http://dx.doi.org/10.1016/S0074-7696(03)01004-0
3. Kafri R, Levy J, Ginzberg MB, Oh S, Lahav G, Kirschner MW. Dynamics extracted from fixed cells reveal feedback linking cell growth to cell cycle. Nature 2013; 494:480-3; PMID:23446419; http://dx.doi.org/10.1038/nature11897
4. Son S, Tzur A, Weng Y, Jorgensen P, Kim J, Kirschner MW, Manalis SR. Direct observation of mammalian cell growth and size regulation. Nat Methods 2012; 9:910-2; PMID:22863882; http://dx.doi.org/10.1038/nmeth.2133
5. Tzur A, Kafri R, LeBleu VS, Lahav G, Kirschner MW. Cell growth and size homeostasis in proliferating animal cells. Science 2009; 325:167-71; PMID:19589995; http://dx.doi.org/10.1126/science.1174294
6. Fantes PA. Control of cell size and cycle time in Schizosaccharomyces pombe. J Cell Sci 1977; 24:51-67; PMID:893551
7. Navarro FJ, Weston L, Nurse P. Global control of cell growth in fission yeast and its coordination with the cell cycle. Curr Opin Cell Biol 2012; 24:833-7; PMID:23182517; http://dx.doi.org/10.1016/j.ceb.2012.10.015
8. Turner JJ, Ewald JC, Skotheim JM. Cell size control in yeast. Curr Biol 2012; 22:R350-9; PMID:22575477; http://dx.doi.org/10.1016/j.cub.2012.02.041
9. Martin SG, Berthelot-Grosjean M. Polar gradients of the DYRK-family kinase Pom1 couple cell length with the cell cycle. Nature 2009; 459:852-6; PMID:19474792; http://dx.doi.org/10.1038/nature08054
10. Moseley JB, Mayeux A, Paoletti A, Nurse P. A spatial gradient coordinates cell size and mitotic entry in fission yeast. Nature 2009; 459:857-60; PMID:19474789; http://dx.doi.org/10.1038/nature08074
11. Breeding CS, Hudson J, Balasubramanian MK, Hemmingsen SM, Young PG, Gould KL. The cdr2(+) gene encodes a regulator of G2/M progression and cytokinesis in Schizosaccharomyces pombe. Mol Biol Cell 1998; 9:3399-415; PMID:9843577; http://dx.doi.org/10.1091/mbc.9.12.3399
12. Kanoh J, Russell P. The protein kinase Cdr2, related to Nim1/Cdr1 mitotic inducer, regulates the onset of mitosis in fission yeast. Mol Biol Cell 1998; 9:3321-34; PMID:9843572; http://dx.doi.org/10.1091/mbc.9.12.3321
13. Morrell JL, Nichols CB, Gould KL. The GIN4 family kinase, Cdr2p, acts independently of septins in fission yeast. J Cell Sci 2004; 117:5293-302; PMID:15454577; http://dx.doi.org/10.1242/jcs.01409
14. Coleman TR, Tang Z, Dunphy WG. Negative regulation of the wee1 protein kinase by direct action of the nim1/cdr1 mitotic inducer. Cell 1993; 72:919-29; PMID:7681363; http://dx.doi.org/10.1016/0092-8674(93)90580-J
15. Parker LL, Walter SA, Young PG, Piwnica-Worms H. Phosphorylation and inactivation of the mitotic inhibitor Wee1 by the nim1/cdr1 kinase. Nature 1993; 363:736-8; PMID:8515817; http://dx.doi.org/10.1038/363736a0
16. Wu L, Russell P. Nim1 kinase promotes mitosis by inactivating Wee1 tyrosine kinase. Nature 1993; 363:738-41; PMID:8515818; http://dx.doi.org/10.1038/363738a0
17. Russell P, Nurse P. The mitotic inducer nim1+ functions in a regulatory network of protein kinase homologs controlling the initiation of mitosis. Cell 1987; 49:569-76; PMID:3453113; http://dx.doi.org/10.1016/0092-8674(87)90459-4
18. Hachet O, Berthelot-Grosjean M, Kokkoris K, Vincenzetti V, Moosbrugger J, Martin SG. A phosphorylation cycle shapes gradients of the DYRK family kinase Pom1 at the plasma membrane. Cell 2011; 145:1116-28; PMID:21703453; http://dx.doi.org/10.1016/j.cell.2011.05.014
19. Saunders TE, Pan KZ, Angel A, Guan Y, Shah JV, Howard M, Chang F. Noise reduction in the intracellular pom1p gradient by a dynamic clustering mechanism. Dev Cell 2012; 22:558-72; PMID:22342545; http://dx.doi.org/10.1016/j.devcel.2012.01.001
20. Wood E, Nurse P. Pom1 and cell size homeostasis in fission yeast. Cell Cycle 2013; 12:3228-36; PMID:24047646; http://dx.doi.org/10.4161/cc.26462
21. Almonacid M, Moseley JB, Janvore J, Mayeux A, Fraisier V, Nurse P, Paoletti A. Spatial control of cytokinesis by Cdr2 kinase and Mid1/anillin nuclear export. Curr Biol 2009; 19:961-6; PMID:19427212; http://dx.doi.org/10.1016/j.cub.2009.04.024
22. Sohrmann M, Fankhauser C, Brodbeck C, Simanis V. The dmf1/mid1 gene is essential for correct positioning of the division septum in fission yeast. Genes Dev 1996; 10:2707-19; PMID:8946912; http://dx.doi.org/10.1101/gad.10.21.2707
23. Hachet O, Bendezú FO, Martin SG. Fission yeast: in shape to divide. Curr Opin Cell Biol 2012; 24:858-64; PMID:23127610; http://dx.doi.org/10.1016/j.ceb.2012.10.001
24. Lee IJ, Coffman VC, Wu JQ. Contractile-ring assembly in fission yeast cytokinesis: Recent advances and new perspectives. Cytoskeleton (Hoboken) 2012; 69:751-63; PMID:22887981; http://dx.doi.org/10.1002/cm.21052
25. Rincon SA, Paoletti A. Mid1/anillin and the spatial regulation of cytokinesis in fission yeast. Cytoskeleton (Hoboken) 2012; 69:764-77; PMID:22888038; http://dx.doi.org/10.1002/cm.21056
26. Celton-Morizur S, Racine V, Sibarita JB, Paoletti A. Pom1 kinase links division plane position to cell polarity by regulating Mid1p cortical distribution. J Cell Sci 2006; 119:4710-8; PMID:17077120; http://dx.doi.org/10.1242/jcs.03261
27. Padte NN, Martin SG, Howard M, Chang F. The cell-end factor pom1p inhibits mid1p in specification of the cell division plane in fission yeast. Curr Biol 2006; 16:2480-7; PMID:17140794; http://dx.doi.org/10.1016/j.cub.2006.11.024
28. Deng L, Moseley JB. Compartmentalized nodes control mitotic entry signaling in fission yeast. Mol Biol Cell 2013; 24:1872-81; PMID:23615447; http://dx.doi.org/10.1091/mbc.E13-02-0104
29. Glynn JM, Lustig RJ, Berlin A, Chang F. Role of bud6p and tea1p in the interaction between actin and microtubules for the establishment of cell polarity in fission yeast. Curr Biol 2001; 11:836-45; PMID:11516644; http://dx.doi.org/10.1016/S0960-9822(01)00235-4
30. Bähler J, Nurse P. Fission yeast Pom1p kinase activity is cell cycle regulated and essential for cellular symmetry during growth and division. EMBO J 2001; 20:1064-73; PMID:11230130; http://dx.doi.org/10.1093/emboj/20.5.1064
31. Beullens M, Vancauwenbergh S, Morrice N, Derua R, Ceulemans H, Waelkens E, Bollen M. Substrate specificity and activity regulation of protein kinase MELK. J Biol Chem 2005; 280:40003-11; PMID:16216881; http://dx.doi.org/10.1074/jbc.M507274200
32. Vilela M, Morgan JJ, Lindahl PA. Mathematical model of a cell size checkpoint. PLoS Comput Biol 2010; 6:e1001036; PMID:21187911; http://dx.doi.org/10.1371/journal.pcbi.1001036
33. Yan J, Ni X, Yang L. Robust cell size checkpoint from spatiotemporal positive feedback loop in fission yeast. BioMed research international 2013; 2013:910941.
34. Coudreuse D, Nurse P. Driving the cell cycle with a minimal CDK control network. Nature 2010; 468:1074-9; PMID:21179163; http://dx.doi.org/10.1038/nature09543
35. Lera RF, Burkard ME. High mitotic activity of Polo-like kinase 1 is required for chromosome segregation and genomic integrity in human epithelial cells. J Biol Chem 2012; 287:42812-25; PMID:23105120; http://dx.doi.org/10.1074/jbc.M112.412544
36. Kawashima SA, Takemoto A, Nurse P, Kapoor TM. A chemical biology strategy to analyze rheostat-like protein kinase-dependent regulation. Chem Biol 2013; 20:262-71; PMID:23438755; http://dx.doi.org/10.1016/j.chembiol.2013.01.003
37. Fotaki V, Dierssen M, Alcántara S, Martínez S, Martí E, Casas C, Visa J, Soriano E, Estivill X, Arbonés ML. Dyrk1A haploinsufficiency affects viability and causes developmental delay and abnormal brain morphology in mice. Mol Cell Biol 2002; 22:6636-47; PMID:12192061; http://dx.doi.org/10.1128/MCB.22.18.6636-6647.2002
38. Arron JR, Winslow MM, Polleri A, Chang CP, Wu H, Gao X, Neilson JR, Chen L, Heit JJ, Kim SK, et al. NFAT dysregulation by increased dosage of DSCR1 and DYRK1A on chromosome 21. Nature 2006; 441:595-600; PMID:16554754; http://dx.doi.org/10.1038/nature04678
39. Wu L, Russell P. Nif1, a novel mitotic inhibitor in Schizosaccharomyces pombe. EMBO J 1997; 16:1342-50; PMID:9135149; http://dx.doi.org/10.1093/emboj/16.6.1342
40. Grallert A, Connolly Y, Smith DL, Simanis V, Hagan IM. The S. pombe cytokinesis NDR kinase Sid2 activates Fin1 NIMA kinase to control mitotic commitment through Pom1/Wee1. Nat Cell Biol 2012; 14:738-45; PMID:22684255; http://dx.doi.org/10.1038/ncb2514
41. Neumann FR, Nurse P. Nuclear size control in fission yeast. J Cell Biol 2007; 179:593-600; PMID:17998401; http://dx.doi.org/10.1083/jcb.200708054

42. Moreno S, Klar A, Nurse P. Molecular genetic analysis of fission yeast Schizosaccharomyces pombe. Methods Enzymol 1991; 194:795-823; PMID:2005825; http://dx.doi.org/10.1016/0076-6879(91)94059-L
43. Bähler J, Wu JQ, Longtine MS, Shah NG, McKenzie A 3rd, Steever AB, Wach A, Philippsen P, Pringle JR. Heterologous modules for efficient and versatile PCR-based gene targeting in Schizosaccharomyces pombe. Yeast 1998; 14:943-51; PMID:9717240; http://dx.doi.org/10.1002/(SICI)1097-0061(199807)14:10<943::AID-YEA292>3.0.CO;2-Y
44. Maundrell K. nmt1 of fission yeast. A highly transcribed gene completely repressed by thiamine. J Biol Chem 1990; 265:10857-64; PMID:2358444
45. Bendezú FO, Vincenzetti V, Martin SG. Fission yeast Sec3 and Exo70 are transported on actin cables and localize the exocyst complex to cell poles. PLoS One 2012; 7:e40248; PMID:22768263; http://dx.doi.org/10.1371/journal.pone.0040248
46. Bendezú FO, Martin SG. Cdc42 explores the cell periphery for mate selection in fission yeast. Curr Biol 2013; 23:42-7; PMID:23200991; http://dx.doi.org/10.1016/j.cub.2012.10.042
47. Kass WAaTD. Snakes: Active contour models. Int J Comput Vis 1988; 1:321-31; http://dx.doi.org/10.1007/BF00133570